Supplemental Information

In vitro membrane reconstitution of the T cell receptor proximal signaling network

Enfu Hui[1,2] & Ronald D. Vale[1,2]

[1]The Howard Hughes Medical Institute and [2]Department of Cellular and Molecular Pharmacology, University of California, San Francisco, San Francisco, California, USA

Correspondence: vale@ucsf.edu

Contents:

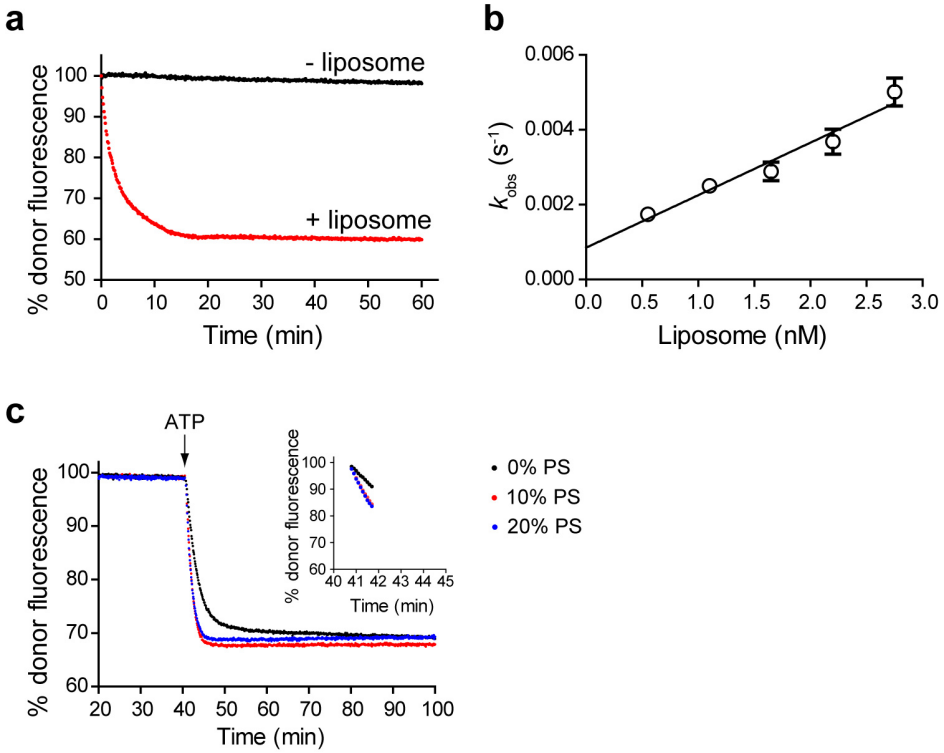

Supplementary Figure 1. Characterization of His_{10}-$SNAP_{505}$•liposomes interaction and the effect of PS on Lck phosphorylation of CD3ζ. **(a, b)** FRET based kinetic analysis of the interaction between His_{10}-$SNAP_{505}$ and Ni^{2+}-NTA-containing liposomes. Purified His_{10}-SNAP was fluorescently-labeled with SNAP-cell 505 (designated as His_{10}-$SNAP_{505}$), which served as a FRET donor for membrane-conjugated rhodamine. Panel **a,** shown in red is the representative time course of fluorescence (excitation: 504 nm; emission: 540 nm) change of 0.25 μM His_{10}-$SNAP_{505}$ upon mixing with 1.1 nM rhodamine-bearing Ni-NTA liposomes, as monitored by a plate reader. Single exponential fitting using Graphpad Prism 5.0 yielded an observed rate constant (k_{obs}) of 0.08 s^{-1}. The black trace corresponds to the fluorescence of His_{10}-$SNAP_{505}$ upon mixing buffer. Panel **b,** k_{obs} measured in **a** plotted as a function of liposome concentration. Assuming pseudo first order kinetics, the elementary rate constants of the binding reaction was determined by linear regression, as previously described[1]. The on-rate (k_{on}) and off-rate (k_{off}) were 1.4×10^6 $M^{-1}s^{-1}$ and 0.0009 s^{-1}, respectively, from which the dissociation constant (K_d) was computed (0.6 nM). Error bars represent s.e.m. from triplicate measurements. **(c)** Inclusion of PS in the membranes moderately accelerated the kinetics of Lck catalyzed phosphorylation of CD3ζ. The time course of CD3ζ phosphorylation was followed by FRET essentially as described in **Fig. 1a,b**. His_{10}-Lck (~280 μm^{-2}) and His_{10}-CD3ζ (~1300 μm^{-2}) were attached to liposomes that contained 10% DGS-NTA-Ni, 0.3% Rhod-PE and indicated molar fractions of PS (at the cost of PC). Shown are representative traces of $SNAP_{505}$-tSH2 fluorescence before and after the addition of ATP, under the three indicated PS content. The inset shows the first 1 min linear phase of the fluorescence changes, allowing the estimation of initial rates of phosphorylation under different conditions. Increasing PS content from 0% to 10% accelerated CD3ζ phosphorylation by 1.8-fold. No further rate enhancement was observed when PS content increased from 10% to 20%. A similar result was obtained in an independent experiment.

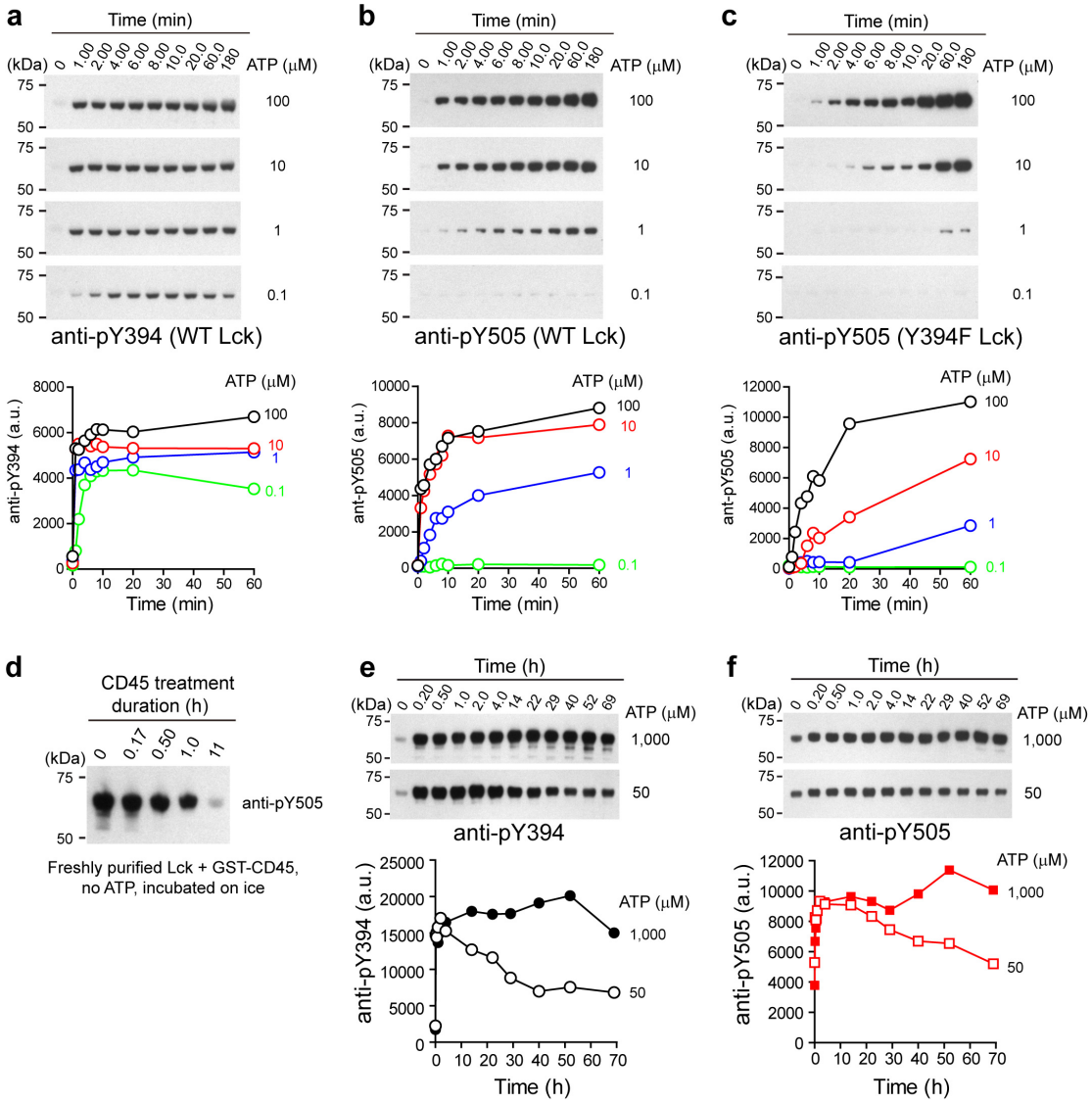

Supplementary Figure 2. Characterization of Lck autophosphorylation and dephosphorylation reactions. (**a-c**) Time course of autophosphorylation of liposome-bound Lck at different ATP concentrations. Panel **a**, immunoblots and a quantification plot showing the kinetics of Y394 phosphorylation at indicated ATP concentrations. Panel **b**, immunoblots and a quantification plot showing the kinetics of Y505 phosphorylation at indicated ATP concentrations. Panel **c**, immunoblots and a quantification plot showing the kinetics of Y505 phosphorylation at indicated ATP concentrations. Unphosphorylated Lck (WT) or Lck (Y394F) was pre-bound to liposomes at ~500 μm^{-2} density, and experiments were conducted at RT essentially as described in **Online Methods**. **(d)** An immunoblot showing the time-dependent dephosphorylation of Lck Y505 by the cytosolic portion of CD45. Freshly purified His_{10}-Lck (10 μM) was incubated with 0.5 μM GST-CD45 on ice for indicated length of time, and then subjected to SDS-PAGE and WB using an mAb against pY505-Lck. (**e,f**) Immunoblots and quantification plots showing the time-dependent changes in phosphorylation of Lck. 5.04 μM His_{10}-Lck (WT) was incubated with indicated concentrations of ATP in solution on ice. Aliquots of reactions were terminated with SDS sample buffer and indicated time points and analyzed for phosphorylation on both Y394 (panel **e**) and Y505 (panel **f**) using phosphospecifc antibodies (**Online Methods**).

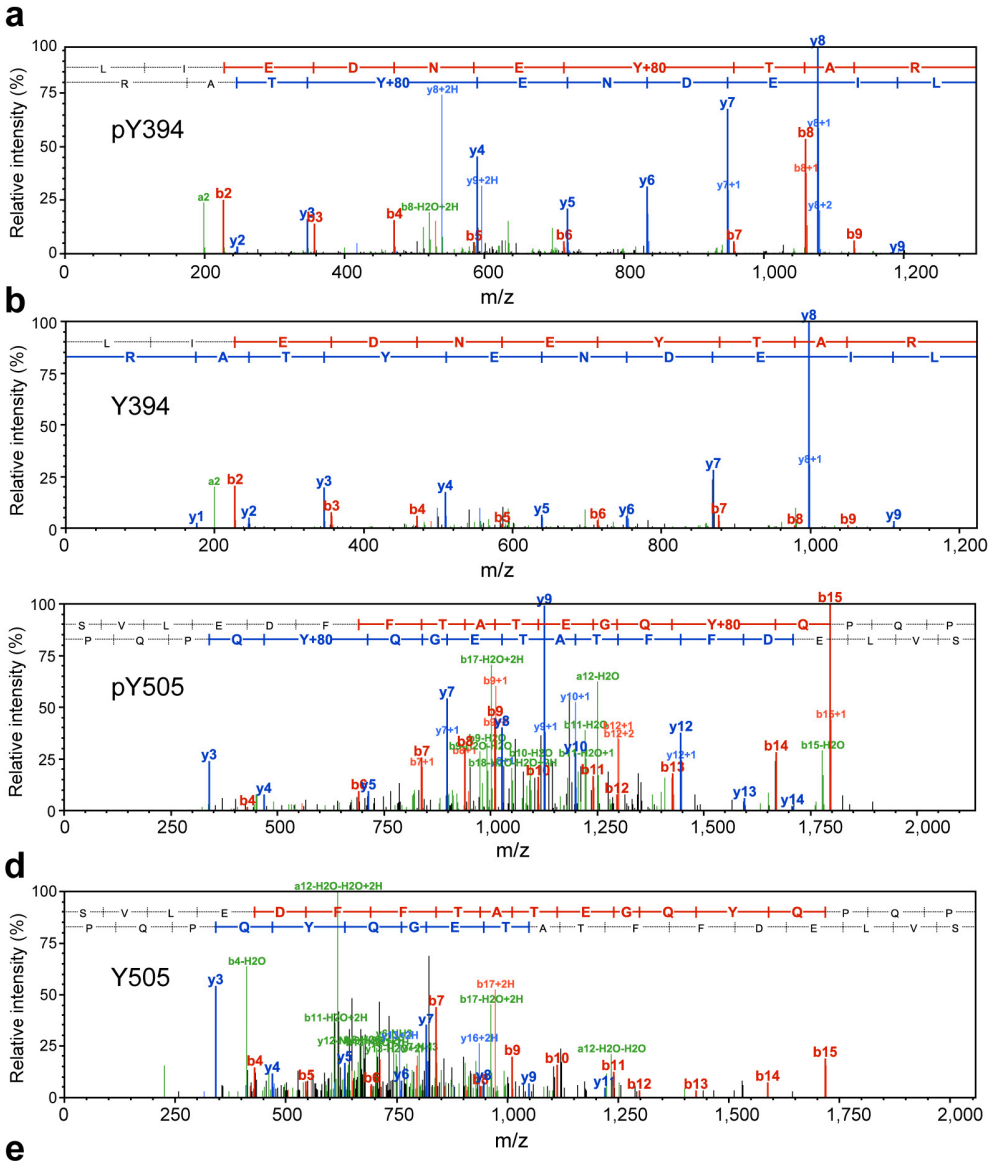

e

	Peptide Sequence	Theoretical Mass [M]	Experimental Mass $[M+2H]^{2+}$	Mass Accuracy (ppm)	*Sequest Xcorr	∑ Total-Ion -Current	Occupancy (%)
pY394	LIEDNEpYTAR	1302.5493	652.2818	1.03	3.50	6.36×10^6	82
Y394	LIEDNEYTAR	1222.5830	612.2982	1.83	3.74	1.41×10^6	
pY505	SVLEDFFTATEGQpYQPQP	2135.9137	1068.9641	0.53	5.00	1.30×10^7	97
Y505	SVLEDFFTATEGQYQPQP	2055.9426	1028.9783	0.80	3.70	3.63×10^5	

Supplementary Figure 3. Quantitation of Lck phosphorylation on both regulatory tyrosines. **(a-d)** Representative fragment ion spectra for peptides containing phosphorylated Y394, unphosphorylated Y394, phosphorylated Y505, and unphosphorylated Y505. LC-MS was carried out as described in **Online Methods**. (**e**) Table summarizing relevant mass spectrometry parameters, which was obtained by using a 3 ppm peptide threshold and >2 Sequest Xcorr score. % occupancy was calculated by dividing the total ion current (TIC) for the phosphorylated peptide by the sum of TIC for both the phosphorylated and unphosphorylated cognate peptide. This TIC based quantification method has been shown to have greater dynamic range than both spectral counting and isotope labeling methods[2,3].

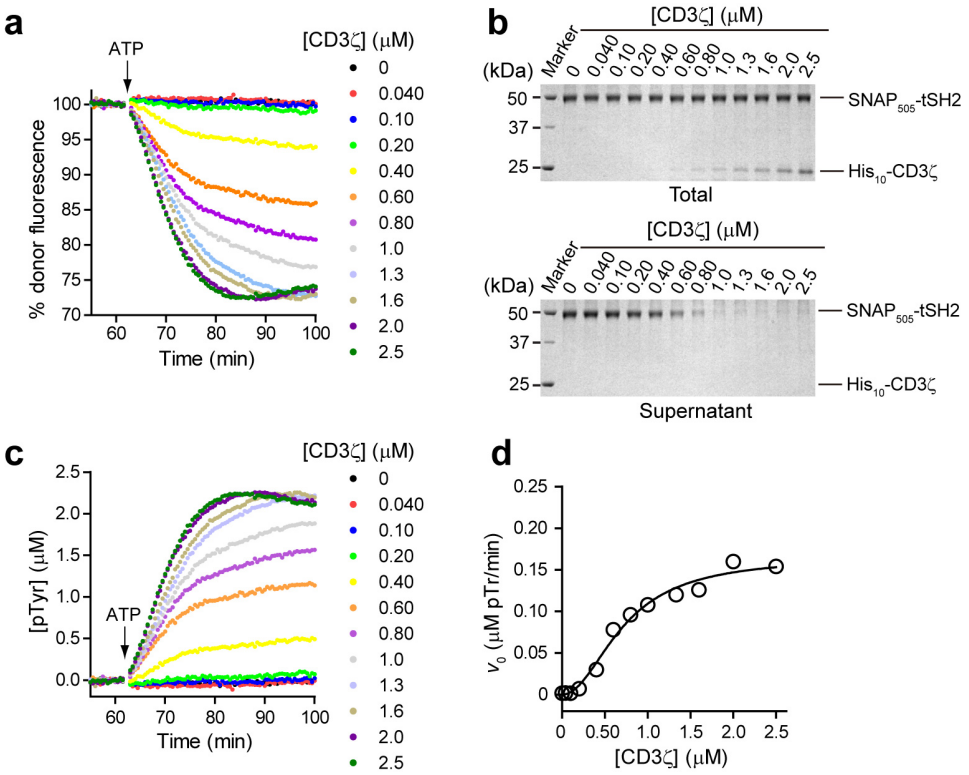

Supplementary Figure 4. Enzyme kinetics for Lck on membranes using CD3ζ as a substrate. **(a)** Representative traces for fluorescence changes of $SNAP_{505}$-tSH2 at different CD3ζ concentrations. Phosphorylation assays were done essentially as described in **Fig. 1a,b**, using $SNAP_{505}$-tSH2 (1.2 μM) as the FRET reporter for ITAM phosphorylation. **(b)** Coomassie-stained SDS-PAGE gels showing the $SNAP_{505}$-tSH2 and CD3ζ in the total (liposome-bound + solution) and solution phase, upon the completion of FRET measurements (t = 100 min). Following FRET measurements, all samples were subjected to liposome sedimentation (278,000g, 20 min), and the supernatant fraction was collected. Equal fractions of the total and supernatant samples were subjected to SDS-PAGE. $SNAP_{505}$-tSH2 was depleted from the supernatant as CD3ζ concentration increased. This experiment also suggests that 100% binding of $SNAP_{505}$-tSH2 to pCD3ζ corresponds to ~28% fluorescence quenching. **(c)** The molar phosphorylation signal plotted as a function of time. The fluorescence signal in **a** was converted to molar phosphorylation signal, assuming each $SNAP_{505}$-tSH2 binding reports phosphorylation of a single ITAM (hence, phospohrylation of a pair of tyrosine residues). (**d**) The initial rate (v_0) of phosphorylation plotted as a function of CD3ζ concentration. v_0 was calculated as the slope of the first 10% increase of the phosphorylation signal for each condition. Note: Lck density (~2.5 μm^{-2}) is two orders of magnitude lower than in **Fig. 2a**, so that the effect of *trans* autophosphorylation on v_0 is minimal.

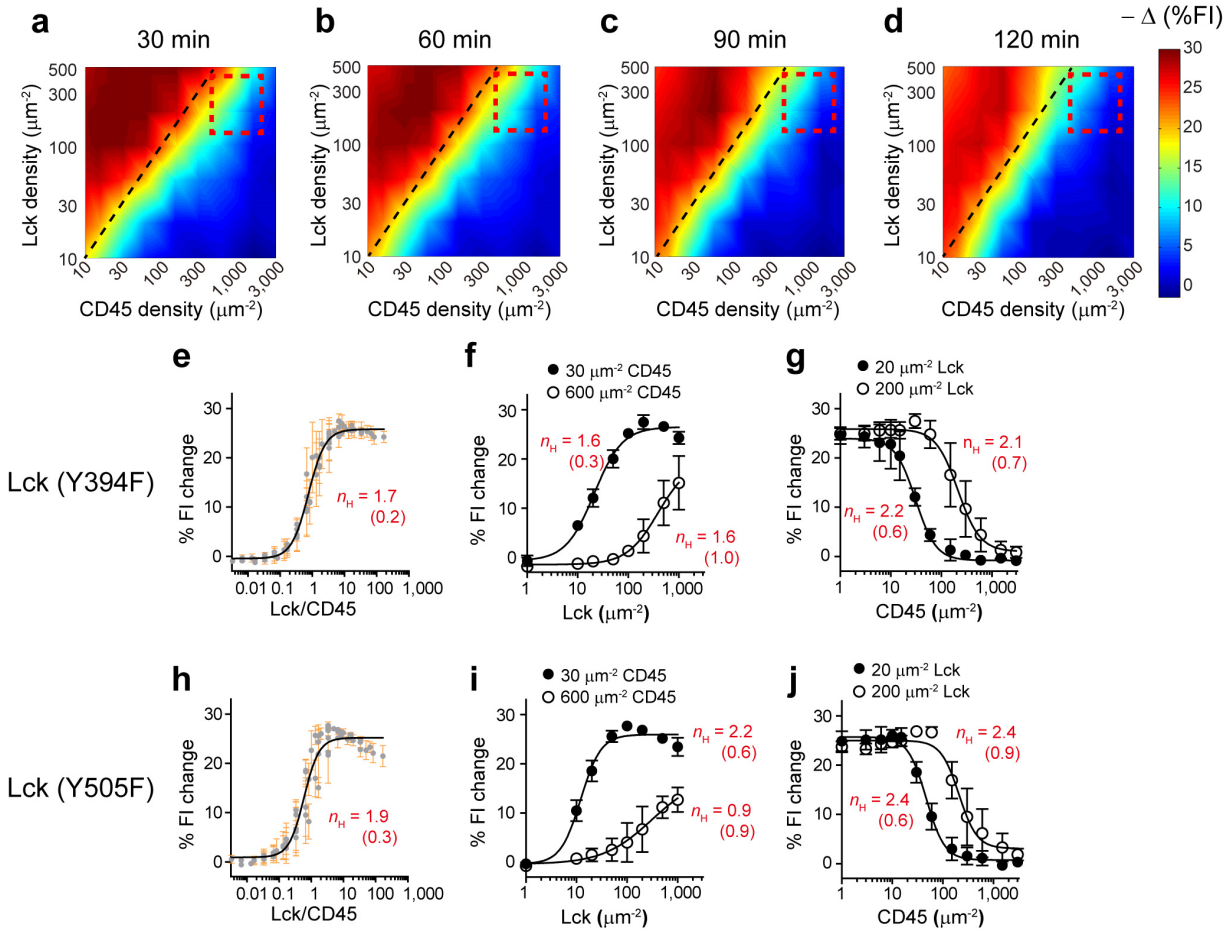

Supplementary Figure 5. Further analyses of the phase diagrams of the membrane reconstituted Lck-CD45-CD3ζ network. **(a-d)** Phase diagrams of the membrane-reconstituted Lck-CD45-CD3ζ network measured at different time points. Liposome reconstitution of Lck (WT) with CD45 and CD3ζ and FRET assays were performed as described in **Fig. 5a,b** and the % donor quenching at 30 min, 60 min, 90 min and 120 min after ATP addition were used to construct heat maps. As in **Fig. 5c**, the black dashed lines indicate conditions with equal molar ratio of Lck and CD45. The red dashed boxes highlight the regime with physiological densities of Lck and CD45. Similar phase diagrams were acquired in another experiment using independent materials. (**e-g**) Dose response plots for Lck (Y394F). FRET data as shown in **Fig. 5b,c** for Lck (Y394F) were plotted in the same manner as for Lck (WT) in **Fig. 5d-f**. **(h-j)** Dose response plots for Lck (Y505F). FRET data as shown in **Fig. 5b,c** for Lck (Y505F) were plotted in the same manner as for Lck (WT) in **Fig. 5d-f**. All data shown in this figure were fit with sigmoidal dose response curves (variable slopes) using Graphpad Prism 5.0 and the Hill-coefficients (n_H) are indicated with s.e.m. in brackets. Error bars represent s.e.m. from three independent measurements.

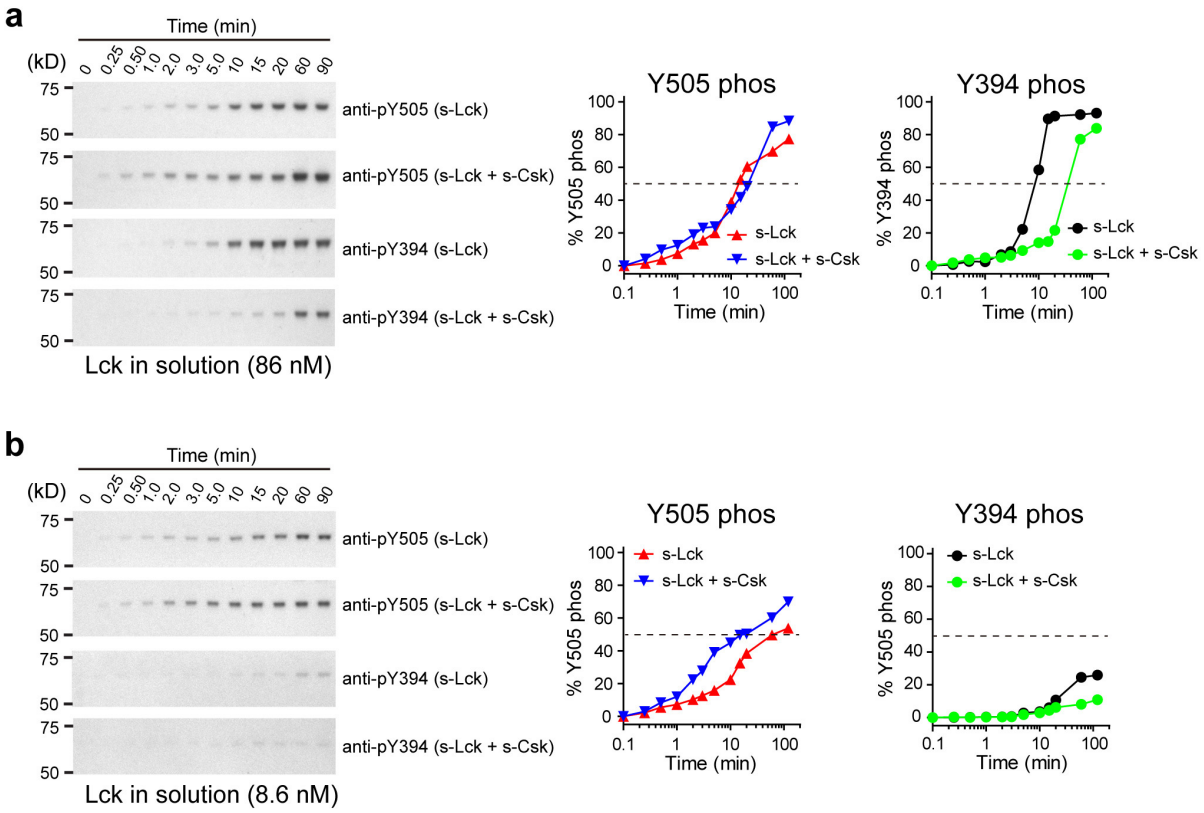

Supplementary Figure 6. Csk affects tyrosine phosphorylations of Lck in solution. **(a)** Left, immunoblots showing the time course of ATP-triggered phosphorylation of Y394 and Y505 of 86 nM Lck in solution, with or without 86 nM Csk. Experiments shown here were essentially the same as **Fig. 6a** except in the absence of liposomes. Right, immunoblots quantified, normalized and plotted against time in a logarithmic scale. pY505 WB signals were and normalized to the last data point (90 min) of the "m-Lck + m-Csk" condition as shown in **Fig. 6a**, and plotted against time in a logarithmic scale; pY394 WB signals were quantified and normalized to the last data point (90 min) of the "m-Lck" condition as shown in **Fig. 6a. (b)** Left, immunoblots showing the time course of ATP-triggered phosphorylation of Lck at 8.6 nM concentration, with or without 86 nM Csk. Experiments shown here were essentially the same as **Fig. 6b** except in the absence of liposomes. Right, quantification plots of immunoblots shown on the left. pY505 WB signals were normalized to the last data point (90 min) of the "m-Lck + m-Csk" condition in **Fig. 6b**; pY394 WB signals were normalized to the last data point (90 min) of the "m-Lck" condition in **Fig. 6b**. For each condition, the WB signal at time zero was arbitrary plotted as a data point at 0.1 min. The dashed lines indicate 50% phosphorylation. All experiments shown here were performed side-by-side with experiments shown in **Fig. 6a,b**. Original images of blots can be found in **Supplementary Fig. 9**.

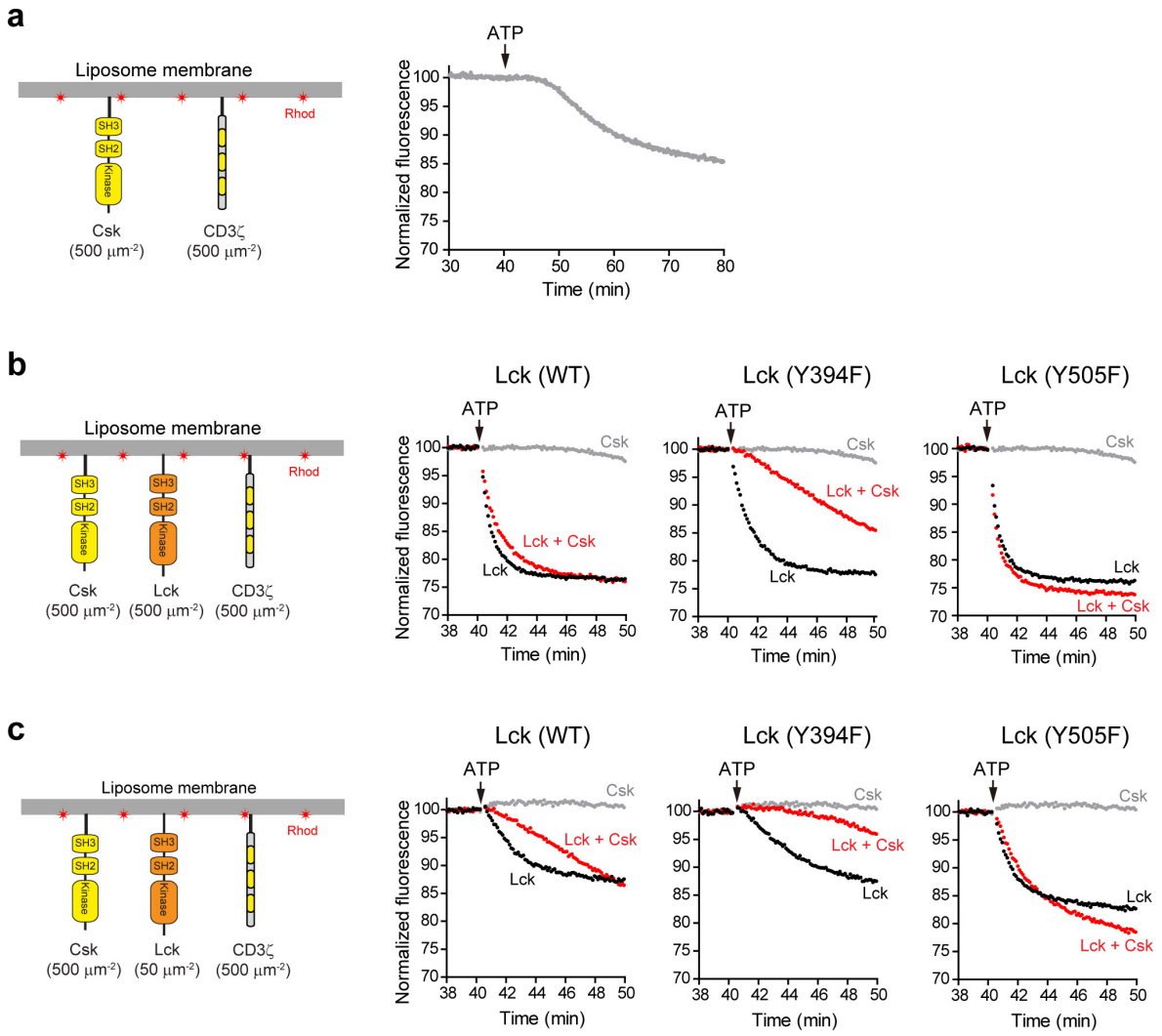

Supplementary Figure 7. Csk directly phosphorylates CD3ζ but retards CD3ζ phosphorylation in the context of Lck. **(a)** Left, a cartoon showing a liposome membrane reconstituted with Csk and CD3ζ (~500 μm^{-2} each). Phosphorylation of CD3ζ was monitored by FRET using SNAP$_{505}$-tSH2 (omitted in the cartoon) as described in **Fig. 1a**. Right, the time course of SNAP$_{505}$-tSH2 fluorescence, before and after the addition of ATP. **(b)** The cartoon on the left shows a liposome membrane reconstituted with equal densities of Csk, CD3ζ and Lck (WT, Y394F, or Y505F mutant). Phosphorylation of CD3ζ was again monitored by FRET. The red traces in the plots corresponds to the the time course of SNAP$_{505}$-tSH2 fluorescence before and after the addition of ATP, when both Lck and Csk were membrane reconstituted with CD3ζ; the black traces corresponds to conditions in which Csk omitted; the grey traces corresponds to conditions in which Lck was omitted. **(c)** Kinetic traces of SNAP$_{505}$-tSH2 fluorescence when experiments as shown in **b** were repeated at lower surface density (~50 μm^{-2}) of Lck. Results shown in this figure were repeatable in an independent measurement.

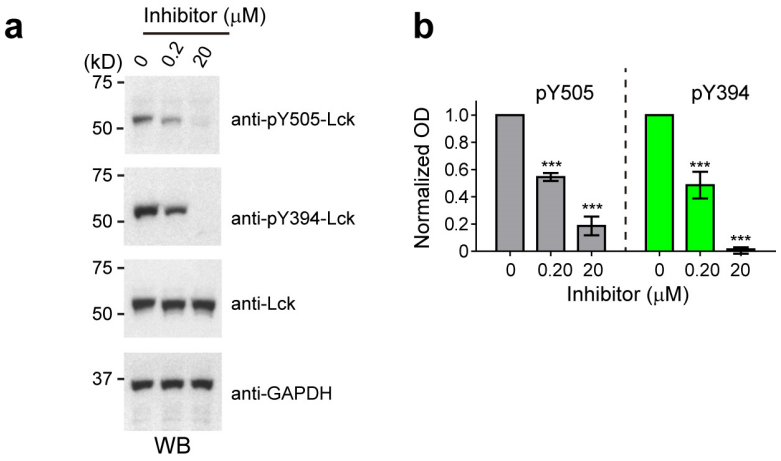

Supplementary Figure 8. Treatment of Jurkat cells with an Lck-specific inhibitor decreased the phosphorylation of Y505. **(a)** Immunoblots showing the effects of Lck specific inhibitor on the phosphorylation of Y505 and Y394 of Lck. Jurkat cells were treated with either 0.2 μM or 20 μM cell-permeable Lck specific inhibitor (IC_{50}: 0.016 μM for Lck and 5.18 μM for Csk[4]) or equal volume of DMSO (indicated as "0 μM") at 37 °C for 0.5 h. Cells were harvested, lysed and subjected to SDS-PAGE, as described in **Online Methods**. Phosphorylation of Y505 and Y394 were immunoblotted using mouse anti-pY505-Lck mAb (558552, BD Phosflow) and rabbit anti-pY416-Src polyclonal Ab (2101S, Cell signaling), respectively. Total Lck and GAPDH levels from the same samples were determined by WB using rabbit anti-Lck polyclonal Ab (2984S, Cell Signaling) and mouse anti-GAPDH mAb (MAB374, Millipore). **(b)** A bar graph showing the quantification of immunoblots shown in **a**. pY505 and pY394 WB signals were quantified, and normalized to the DMSO control condition. Error bars represent s,d. from triplicate determination. Statistical significance was evaluated by one-sided Student's t test, *** $p < 0.001$.

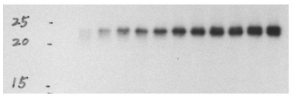
Fig. 1c
(anti-pY142-ζ, + SH2)

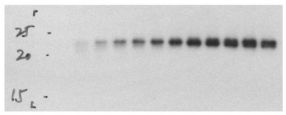
Fig. 1c
(anti-pY142-ζ, – SH2)


Fig. 2a
(anti-pY394, solution)

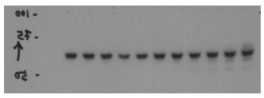
Fig. 2a
(anti-pY394, membrane)

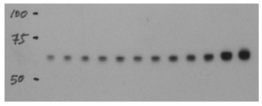
Fig. 2a
(anti-pY505, solution)

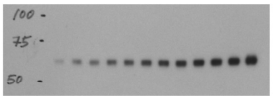
Fig. 2a
(anti-pY505, membrane)

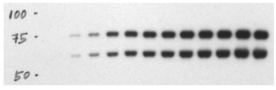
Fig. 2b
(anti-pY505)

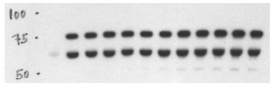
Fig. 2b
(anti-pY394)

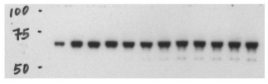
Fig. 2c
(anti-pY394, Lck WT)

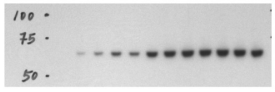
Fig. 2c
(anti-pY505, Lck WT)

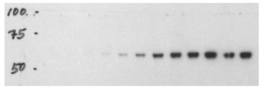
Fig. 2c
(anti-pY505, Lck Y394F)

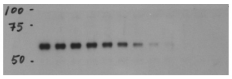
Fig. 4a
(anti-pY394-Lck)

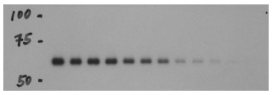
Fig. 4a
(anti-pY505-Lck)


Fig. 4a
(anti-pY142-ζ, no tSH2)

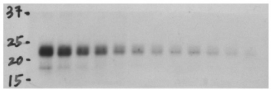
Fig. 4a
(anti-pY142-ζ, 0.1 μM tSH2)

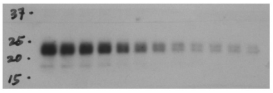
Fig. 4a
(anti-pY142-ζ, 0.5 μM tSH2)

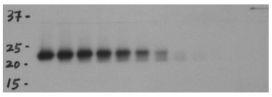
Fig. 5g
(anti-pY142-ζ, – tSH2)

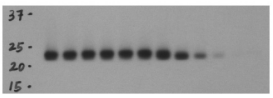
Fig. 5g
(anti-pY142-ζ, + tSH2)

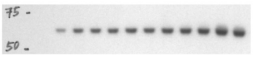
Fig. 6a
(anti-pY505, m-Lck)


Fig. 6a
(anti-pY505, m-Lck + m-Csk)

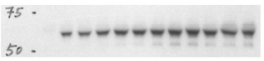
Fig. 6a
(anti-pY394, m-Lck)

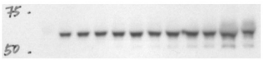
Fig. 6a
(anti-pY394, m-Lck + m-Csk)


Fig. 6b
(anti-pY505, m-Lck)


Fig. 6b
(anti-pY505, m-Lck + m-Csk)

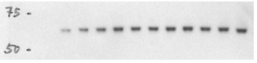
Fig. 6b
(anti-pY394, m-Lck)

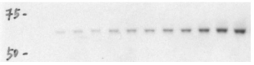
Fig. 6b
(anti-pY394, m-Lck + m-Csk)

Supplementary Figure 9. Uncropped immunoblots with molecular weight markers.

Supplementary Note. A review of studies on how tyrosine phosphorylation regulates the activities of SFKs.

Multiple lines of evidence have suggested that the catalytic activities of SFKs are regulated by phosphorylation of two conserved tyrosines: one in the activation loop of the kinase domain which leads to kinase activation and the other at the C terminal tail which inhibits kinase activity[5]. While this general model is widely cited, the biochemical data in the literature that supports this model shows discrepancies among different studies.

c-Src is the best characterized SFKs, and its regulatory mechanism has received much attention over the last three decades. In 1985, Courtneidge[6] showed that c-Src immunoprecited from cells that were pretreated with the phosphatase inhibitor vanadate exhibited a higher level of phosphorylation and a weaker kinase activity towards enolase compared with c-Src from untreated cells (Figure 5 of reference herein). This study provided the first *in vitro* evidence that phosphorylation of c-Src might downregulate its activity. Consistent with this finding, Cooper and King directly showed that immunoprecipitated c-Src substantially increased its kinase activity by 10-20 fold after treatment with phosphatase[7] (Figure 1 of reference herein). A later study by Kmiecik et al., however, obtained the opposite result that phosphatase inhibition (with vanadate treatment) increased the activity of WT c-Src immunoprecipitated from c-Src overexpressing cells, but became inhibitory when the Y416F mutant was used[8] (Figure 2 of reference herein). However, interpretation and comparison of the results from these two studies is complicated by the fact that the exact phospho-enzyme composition in these experiments was not determined and vanadate, phosphatase, or autophosphorylation would be expected to alter phosphorylation levels of both Y527 and Y416. Furthermore, the cell type used for the immunoprecipitation studies might affect the outcome, since phosphorylation of Y416 is low in normal cells, but becomes substantial in cells overexpressing c-Src[8] or cells that undergo transformation[9].

In 1987, three groups studied in more detail how tyrosine mutations alter the activity of c-Src. Piwnica-Worms et al. found that the Y527F mutation increased kinase activity by 9.4-fold[10] (Figure 1 of reference herein), while the Y416F mutation enhanced the activity by 1.3-fold, and the double mutation (Y416F/Y527F) increases the activity by 5.0-fold[10] (Figure 5 of reference herein). Similarly, Shalloway and colleagues found that Y527F mutation increased c-Src activity by 13-fold, while Y416F mutation did not alter the activity of c-Src, and the double mutation (Y416F/Y527F) increased the activity by 6.6-fold[11] (Table 1 of reference herein). In a third study from Cartwright et al., Y527F was found to increase c-Src activity by 5-10 fold using a similar *in vitro* assay (Figure 3 of reference herein)[12].

The general picture emerging from the three studies in 1987 is that Y527F mutation increases the activity of immunoprecipitated c-Src, whereas Y416F mutation has little, if any, effect on the kinase activity. However, in the following year, Shalloway and colleagues reported that Y416F mutation decreased the activity of v-Src by 80% (Figure 3 of reference herein)[8], suggesting that phosphorylation of Y416 upregulates the kinase activity. Therefore, Y416 phosphorylation appeared to have distinct effects on c-Src and v-Src activities. Notably, v-Src does not contain the C terminal inhibitory tyrosine as c-Src does (Y527). Y416 of v-Src was also found to be strongly phosphorylated *in vivo*, in contrast to the low level of phosphorylation of this tyrosine in c-Src from normal cells[13]. This different extent in Y416 phosphorylation may explain why Y416F has a greater impact on v-Src activity than on c-Src.

To our knowledge, there were two mutational studies on this topic for Lck. In 1988, Amrein and Sefton reported that Y505F mutation only slightly increases the *in vitro* activity of Lck that was immunoprecipitated from cell lysate[14] (cited as unpublished observation in the referenced study). As this result contrasted the previously reported strong activating effect of Y527F mutation on c-Src[10-12], it

suggested that the degree of activity regulation by tyrosine phosphorylation can vary between members of SFKs. In 1996, D'Oro et al. re-examined how tyrosine mutations alter the catalytic activity of Lck using a short peptide derived from cdc2 as the substrate[15]. Lck mutants were expressed and immunoprecipitated from either $CD45^-$ or $CD45^+$ cell lines and examined with a single time end point assay. Immunoprecipitated Lck (Y505F) had higher kinase activity than WT Lck, whereas Lck (Y394F) and the double tyrosine mutant (Y394F/Y505F) had much lower activity than WT Lck (Figure 4 and Figure 5 of reference herein). These results were in sharp contrast to previous *in vitro* studies on c-Src[10,11], which showed that Y416F (analogous to Y394F in Lck) has very little impact on c-Src activity, and the double mutation (Y416F/Y527F) increases the activity by at least 5-fold.

In vitro studies on how tyrosine phosphorylation regulates SFKs using recombinant, purified proteins also exist. While earlier work listed above relied solely on tyrosine mutations for studying phospho-regulation of SFKs, more recent work attempted to generate different phospho-forms of SFKs from purified proteins, employing either their autophosphorylation activities or the inhibitory kinase Csk.

In 1996, the Knight group took advantage of the autophosphorylation activity of Src to produce the prephosporylated kinase[16]. They showed prephosphorylation of Src decreases the activity by 80%. However, while the phosphorylation on the inhibitory tyrosine appeared high, the phosphate occupancy on the activating tyrosine was variable.

In the following year, Moarefi et al. purified the C terminally phosphorylated Hck from SF9 cells, by coexpressing the Hck with Csk[17]. It was found that this phosphorylated Hck greatly reduces the activity as compared to the unphosphorylated kinase (Figure 1c of reference herein), and that addition of a high-affinity SH3 ligand strongly activates the kinase. The precise fold of activity changes was not reported.

In 2000, Porter et al. found that preincubation of Hck with ATP increases the catalytic activity by 2.6-fold[18] (Table 2 of the reference herein). However, this was solely attributed to the phosphorylation on the activating tyrosine (Y416), because this previous work completely ignored the autophosphorylation on the C terminal inhibitory tyrosine, which also undergoes autophosphorylation, as shown previously for Src by other groups and for Lck in the current study.

A more recent study by Nika et al. approached the question from a different angle. They took advantage of the phospho-specific antibodies against regulatory tyrosines to sort Lck molecules into different populations based on their phosphorylation states through immunoprecipitation and compared the catalytic activities of these Lck subpopulations in an end-point assay (Figure 4 of reference herein). This work revealed that immunoprecipitated Y394 phosphorylated Lck (which is a mixture of monophosphorylated Lck-pY394 and doubly phosphorylated Lck-pY394, pY505) is ~5-fold more active than Lck that is not phosphorylated on this tyrosine (a mixture of unphosphorylated form Lck (Apo) and Y505 monophosphorylated form Lck-pY505). They also found that the doubly phosphorylated Lck-pY394, pY505) and monophosphorylated Lck-pY394 exhibit similar activity. This study has provided a better understanding on the regulatory effects of Lck tyrosine phosphorylations but this study did not determine the catalytic activity of the unphosphorylated Lck, which provides critical reference point for such comparisons. Furthermore, the Y505 monophosphorylated form (Lck-pY505) was not prepared and analyzed.

In conclusion, these aforementioned studies established a strong correlation between tyrosine phosphorylation and the changes in the catalytic activity of SFKs. However, there are many discrepancies between studies in the literature which are difficult to resolve and the magnitudes of

phospho-regulation in SFKs are still controversial (e.g. for the phosphorylation of the activating tyrosine (Y416 in Src and Y394 in Lck).

In our opinion, these discrepancies could arise from several parameters in which prior experiments were conducted. First, and perhaps the most notable, is the lack of homogeneous, pure populations of different phospho-SFKs that were used in the enzymatic assays. SFKs can exist in at least four states due to the presence of two regulatory tyrosines: unphosphorylated, two monophophorylated species (either on the activating or inhibitory tyrosine), and doubly phosphorylated states. Thus these four forms of the enzyme must be isolated from one another and assayed in completely dephosphorylated and phosphorylated states, yielding a matrix of four measurements for comparison. However, such comparison has not been done and is difficult to achieve using immunoprecipitated SFKs. Nika et al., for example, showed that four phospho-forms of Lck exist at comparable levels in Jurkat cells[19]. Hence, the measured activity of the immunoprecipitated WT kinase would be the weighted average of all these states, rather than the real activity of the unphosphorylated kinase, and this might depend upon the cell type, culturing condition and immunoprecipitation procedures. These variables could potentially explain some of the discrepancies between different studies as mentioned above. A second source of variability and potential for nonphysiological interpretation are the substrates used in the kinase reactions, which have used acid-denatured enolase[6-12], angiotensin[14] and a synthetic peptides[15,17,18]. In none of these studies was a natural SFK substrate used in the reaction. Third, most studies cited above measured end point substrate phosphorylation at a single substrate concentration. These assays did not provide information on k_{cat} and K_M, which require the measurement of initial rate (v_o) at a series of substrate concentration by kinetic assays. A single end point measurement also can subject to more variability than multi-time point kinetic measurements. Fourth, many studies on SFK regulation involved immunoprecipitation reactions, where the enzyme is bound and crosslinked by antibodies, which might quantitatively influence the enzyme reaction. Additional proteins are also likely present in these immunoprecipitations. Lastly, while solution measurements are likely to represent a more native environment for enzyme-substrate interactions than immunoprecipitates from cell lysates, SFKs operate on membranes rather than in cytoplasm. As we show here, the 2-D membrane environment dramatically accelerates enzyme reaction rates compared with a 3-D solution.

Supplementary References:

1. Davis, A.F. et al. Kinetics of synaptotagmin responses to Ca2+ and assembly with the core SNARE complex onto membranes. *Neuron* 24, 363-76 (1999).

2. Yang, X., Friedman, A., Nagpal, S., Perrimon, N. & Asara, J.M. Use of a label-free quantitative platform based on MS/MS average TIC to calculate dynamics of protein complexes in insulin signaling. *J Biomol Tech* 20, 272-7 (2009).

3. Asara, J.M., Christofk, H.R., Freimark, L.M. & Cantley, L.C. A label-free quantification method by MS/MS TIC compared to SILAC and spectral counting in a proteomics screen. *Proteomics* 8, 994-9 (2008).

4. Burchat, A.F. et al. Pyrrolo[2,3-d]pyrimidines containing an extended 5-substituent as potent and selective inhibitors of lck II. *Bioorganic & Medicinal Chemistry Letters* 10, 2171-2174 (2000).

5. Roskoski, R., Jr. Src kinase regulation by phosphorylation and dephosphorylation. *Biochem Biophys Res Commun* 331, 1-14 (2005).

6. Courtneidge, S.A. Activation of the pp60c-src kinase by middle T antigen binding or by dephosphorylation. *Embo J* 4, 1471-7 (1985).

7. Cooper, J.A. & King, C.S. Dephosphorylation or antibody binding to the carboxy terminus stimulates pp60c-src. *Mol Cell Biol* 6, 4467-77 (1986).

8. Kmiecik, T.E., Johnson, P.J. & Shalloway, D. Regulation by the autophosphorylation site in overexpressed pp60c-src. *Mol Cell Biol* 8, 4541-6 (1988).

9. Cartwright, C.A., Kaplan, P.L., Cooper, J.A., Hunter, T. & Eckhart, W. Altered sites of tyrosine phosphorylation in pp60c-src associated with polyomavirus middle tumor antigen. *Mol Cell Biol* 6, 1562-70 (1986).

10. Piwnica-Worms, H., Saunders, K.B., Roberts, T.M., Smith, A.E. & Cheng, S.H. Tyrosine phosphorylation regulates the biochemical and biological properties of pp60c-src. *Cell* 49, 75-82 (1987).

11. Kmiecik, T.E. & Shalloway, D. Activation and suppression of pp60c-src transforming ability by mutation of its primary sites of tyrosine phosphorylation. *Cell* 49, 65-73 (1987).

12. Cartwright, C.A., Eckhart, W., Simon, S. & Kaplan, P.L. Cell transformation by pp60c-src mutated in the carboxy-terminal regulatory domain. *Cell* 49, 83-91 (1987).

13. Smart, J.E. et al. Characterization of sites for tyrosine phosphorylation in the transforming protein of Rous sarcoma virus (pp60v-src) and its normal cellular homologue (pp60c-src). *Proc Natl Acad Sci U S A* 78, 6013-7 (1981).

14. Amrein, K.E. & Sefton, B.M. Mutation of a site of tyrosine phosphorylation in the lymphocyte-specific tyrosine protein kinase, p56lck, reveals its oncogenic potential in fibroblasts. *Proc Natl Acad Sci U S A* 85, 4247-51 (1988).

15. D'Oro, U., Sakaguchi, K., Appella, E. & Ashwell, J.D. Mutational analysis of Lck in CD45-negative T cells: dominant role of tyrosine 394 phosphorylation in kinase activity. *Mol Cell Biol* 16, 4996-5003 (1996).

16. Boerner, R.J. et al. Correlation of the phosphorylation states of pp60c-src with tyrosine kinase activity: the intramolecular pY530-SH2 complex retains significant activity if Y419 is phosphorylated. *Biochemistry* 35, 9519-25 (1996).

17. Moarefi, I. et al. Activation of the Src-family tyrosine kinase Hck by SH3 domain displacement. *Nature* 385, 650-3 (1997).

18. Porter, M., Schindler, T., Kuriyan, J. & Miller, W.T. Reciprocal regulation of Hck activity by phosphorylation of Tyr(527) and Tyr(416). Effect of introducing a high affinity intramolecular SH2 ligand. *J Biol Chem* 275, 2721-6 (2000).

19. Nika, K. et al. Constitutively active Lck kinase in T cells drives antigen receptor signal transduction. *Immunity* 32, 766-77 (2010).